Alexandria Engineering Journal (2011) **50**, 313–320

Alexandria University

Alexandria Engineering Journal

www.elsevier.com/locate/aej
www.sciencedirect.com

ORIGINAL ARTICLE

A new beam-column model for seismic analysis of RC frames – Part I: Model derivation

El-Sayed Mashaly, Mohamed El-Heweity *, Hamdy Abou-Elfath, Mostafa Ramadan

Structural Eng. Dept., Faculty of Engineering, Alexandria University, Alexandria, Egypt

Received 3 April 2011; accepted 4 December 2011
Available online 5 February 2012

KEYWORDS

Beam-column models;
Reinforced Concrete;
Seismic analysis;
Inelastic analysis;
Frame structures

Abstract In this study, a reliable and computationally efficient beam-column model is proposed for seismic analysis of Reinforced Concrete (RC) frames. The model is a simplified version of the Flexibility-Based Fiber Models (FBFMs), which rely on dividing the element length into small segments and dividing the cross section of each segment into concrete and steel fibers. In the proposed model, only the two end sections are subdivided into fibers and uniaxial material models that consider the various behavioral characteristics of steel and concrete under cyclic loading conditions are assigned for the cross section fibers.

The proposed model is simpler than the FBFMs as it does not require monitoring the responses of many segments along the element length, which results in a significant reduction in computations. The inelastic lengths at the ends of the proposed model are divided into two inelastic zones; cracking and yielding. The inelastic lengths vary according to the loading history and are calculated in every load increment. The overall response of the RC member is estimated using preset flexibility distribution functions along the element length. A flexibility factor η is utilized to facilitate selecting the proper flexibility distribution shape. The proposed model is implemented into the computer program DRAIN-2DX.

* Corresponding author.
E-mail address: heweity@hotmail.com (Mohamed El-Heweity).

Peer review under responsibility of Faculty of Engineering, Alexandria University.
doi:10.1016/j.aej.2012.01.003

Production and hosting by Elsevier

1. Introduction

Intense research has been dedicated in the last few decades to the development of beam-column models to predict the inelastic seismic response of RC frame structures with a reasonable balance between accuracy and efficiency. Improving the accuracy of beam-column models often increases their computational demands and may reduce their efficiency. Seismic evaluation of frame structures often requires repeated solutions of the response of multi-degrees of freedom systems. The computations

involved in such evaluation can become excessive and simplicity of the modeling approach may be an important issue to accomplish the analysis in a reasonable time.

Beam-column models can be represented using two main modeling approaches in accordance with the increasing level of complexity. The first is global modeling, where each RC member is modeled as one element and the second is microscopic modeling, where the members are divided into a large number of finite elements.

Microscopic modeling is suitable only for studying critical regions, since it is computationally expensive for the seismic analysis of multi-story frames. Global modeling, on the other hand, represents the best compromise between simplicity and accuracy as it provides a considerable information on the seismic inelastic response of frame structures in a reasonable time.

Global beam-column models, which are the focus of this study, can be divided into two types: (a) Lumped Plasticity Models (LPMs), and (b) Distributed Plasticity Models (DPMs). LPMs rely on the fact that the inelasticity of the RC frames under seismic excitation often concentrates at the member ends. Thus, an early approach to model this behavior was by means of zero length plastic hinges in the form of non-linear springs located at the member ends. The hysteretic force–deformation relations of these end springs are usually based on phenomenological rules. Examples of the LPMs include the two-component model of Clough et al. [1] and the one-component model of Giberson [2].

The two-component model consists of two components acting in parallel. The first component is linear elastic to represent strain-hardening, while the second component is elastic perfectly plastic to represent the plastic deformations concentrated in plastic hinges at the element ends. The one-component model, on the other hand, consists of two non-linear rotational springs attached in series at the ends of an elastic element. This model is more popular than the two-component model because of its simplicity as well as its ability of describing more complex hysteretic behavior by the selection of proper moment–rotation relations for the end springs.

Several hysteretic rules with empirical control parameters are proposed to describe the moment–rotation relationships of the non-linear springs. Examples of these rules include Takeda et al. [3], Park et al. [4] and Otani [5]. Typically, these hysteretic rules are based on experimental data obtained by testing of RC sub-assemblages.

A third type of LPMs is the fiber hinge model [6,7], which relies on using inelastic zero-length hinge element at each end of the RC member. The hinge element consists of a number of axial springs that represent the force–displacement relations of the reinforcing steel and the concrete. This approach is capable of simulating the axial–flexural interaction in RC members in a more rational way than the one- and the two component models.

The basic advantage of the LPMs is their simplicity that reduces computations and storage requirements along with improving the numerical stability. However, most LPMs oversimplify certain important aspects of the cyclic behavior of RC members such as the post-yield response and the axial–flexural interaction which could produce inaccurate results. Moreover, the use empirical control parameters in the LPMs limits their generality as the values of these parameters are usually selected by trail and error to produce model response that fit with experimental results of a limited number of RC components.

In the DPMs, material non-linearity can take place at any section along the length of the RC member and the element behavior is derived by integrating the section responses. This results in a more accurate description of the inelastic behavior of RC members. DPMs can be classified into two types, namely, curvature spring models and fiber models.

Curvature spring models include the model proposed by Meyer et al. [8] and later modified by Roufaiel and Meyer [9]. In this model, two springs are considered at the member ends to represent the moment–curvature relations of the end sections. The monotonic moment–curvature relation is derived with ignoring the concrete tensile strength. The hysteretic response is based on phenomenological rules that account for the behavioral characteristics of RC members under cyclic loading. The inelastic lengths at member ends are calculated in every load increment based on the assumption of linear distribution of bending moments along the element length. The element response is determined by assuming a uniform distribution of flexibility along the lengths of the plastic zones.

Another example of the curvature spring models is the model proposed by Park et al. [10]. In this model, the monotonic moment–curvature relationship is derived with considering the concrete tensile strength, while the element response is determined by assuming a linear distribution of flexibility along the lengths of the inelastic zones. The main limitations of the curvature spring models are in oversimplifying the axial–flexural interaction and the flexibility distribution along the plastic hinge regions.

Fig. 1 shows a member idealization in the fiber models, where the element is subdivided into segments distributed along the member length, and the cross section of each segment is subdivided into steel and concrete fibers. The section response is determined by integrating the uniaxial stress–strain relations of the fibers. In practice, only the behavior of a limited number of segments at each end of the member is monitored. Two types formulations are used in the fiber models, the first is displacement-based (stiffness-based) and requires a predefined displacement shape-function to interpolate the displacements along the element length with respect to the nodal displacements and the second is force-based (flexibility-based) and requires using interpolation functions to estimate the forces along the element length with respect to the nodal forces.

Taucer et al. [11] stated that the most promising models for non-linear analysis of RC members are the flexibility based fiber models. Several Flexibility-Based Fiber Models are proposed for seismic analysis of RC members. Examples of theses models include, Kaba and Mahin [12] and Taucer et al. [11]. The only limitation associated with the fiber approach when used for modeling of RC frame members is the substantial amount of computations required for monitoring the responses of several cross sections along the element length and the responses of several fibers over each cross section. On

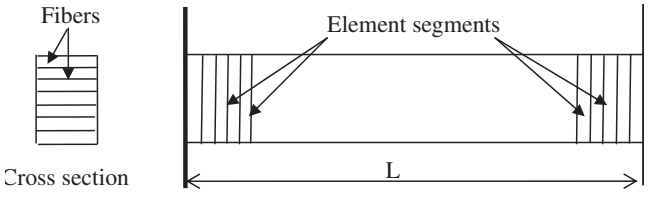

Figure 1 The fiber beam-column model.

the other hand, the fiber approach has many advantages, which include: (a) accounting rationally for the moment–flexural interaction, (b) providing the strains of the fibers as an output during seismic response which can be used for in seismic damage evaluation of RC members, and (c) accounting for the spread of plasticity both over the cross sections and along the member length.

This study proposes a simplified FBFM that requires monitoring only the fiber responses of the end sections of the RC member. The proposed model eliminates the need for monitoring the responses of many segments distributed along the member length which results in a significant reduction in computations. In the proposed model, yielding and cracking lengths at each end are calculated every load increment. The member overall response is estimated using a preset flexibility distribution functions along the element length. A flexibility factor (η) is utilized to facilitate selecting the proper flexibility distribution shape. The proposed model is implemented into the computer program DRAIN-2DX [13].

2. Derivation of the beam-column model

The proposed RC beam-column model is flexibility-based and relies on using force interpolation functions that satisfy equilibrium of moment and axial forces along the element length. A uniform distribution of axial forces and a linear distribution of bending moments are considered in the current study. The assumption of linear distribution of moments along the RC member is correct in case of frames subjected to lateral loads only. The presence of gravity loads will alter the distribution, and in cases of significant gravity loads, the members should be subdivided to capture the moment variation. Also, in this study, the member deformations are assumed small and plane sections are assumed to remain plane and normal to the member longitudinal-axis after deformation. The effect of bond-slip, shear deformation, and the difference in material properties between concrete core and cover are ignored.

The end sections are divided into concrete and steel fibers and a uniaxial stress–strain relation is assigned for each fiber. The tangent section stiffness matrix is derived from the fiber responses which are updated at each load increment based on the applied strain increments. The tangent section flexibility matrix is calculated by inverting of the tangent stiffness matrix.

The member flexibility matrix is calculated based on the end section flexibility coefficients and the preset flexibility distribution functions along inelastic zones. The preset flexibility distribution functions are selected to fit the actual flexibility distributions. The inelastic zones at the member ends are divided into cracking and yielding zones with their lengths are updated in every load increment. The member tangent–stiffness matrix is calculated by inverting of the member tangent–flexibility matrix. A more detailed description of the model derivation is presented in the following sections.

3. Inelastic lengths

Under the effect of lateral loading, the inelastic deformations of the beam-column element are distributed along increasing inelastic zones at the member two ends as shown in Fig. 2. Cracking and yielding lengths at the inelastic zones are calculated based on the distribution of the applied moment and the levels of cracking and yielding moments of the cross section.

The cracking stage arises when the acting moments at the member two ends exceed the section cracking-moment as shown in Fig. 3a. The flexural flexibility of the cracked sections increases with the increase of number of cracked fibers. The cracking length X_{cj} (j = 1 for the left end and 2 for the right end) specifies the portion of the element length where the acting moment is greater than the cross section cracking moment M_c but less than the cross section yielding moment M_y. The cracking length X_{cj} is first calculated for the current moment distribution, and then checked with the previous maximum cracking length, where the current cracking length cannot be smaller than the previous maximum value regardless of the current moment distribution. The cracking length X_{cj} of the plastic region at node j is calculated in terms of the applied end moments (M_1 and M_2), the cross section cracking moment M_c and the member length L, as follow:

$$X_{cj} = \frac{M_j - M_c}{M_1 + M_2} L \tag{1}$$

The yielding stage initiates when the applied moment exceeds the cross section yielding-moment as shown in Fig. 3b. The yielding length X_{yj} specifies the portion of the element length where the acting moment is greater than the section yielding moment M_y. The procedure applied for the calculation of X_{yj} is based on the approach proposed by Abou-Elfath [14]. The calculation approach is illustrated in Fig. 4, which shows a frame member subjected to cyclic loading with M_1 and M_2 are the applied end moments. M_y is the moment that causes initial yielding of the end section in the first loading cycle. In any subsequent loading cycle, the existing of residual fiber strains often causes the formation of a subsequent yield moment M_s different from the initial yield moment M_y. X_p is the maximum plastic length occurred in the previous loading cycle. The yielding length is calculated by defining the intersection point between the applied moment diagram and the yield surface as:

$$\begin{aligned} X_{yj} &= \frac{M_j - M_y}{(M_1 + M_2)X_p + M_y - M_s} L, \quad X_{yj} \le X_p \\ X_{yj} &= \frac{M_j - M_y}{M_1 + M_2} L, \qquad X_{yj} \ge X_p \end{aligned} \tag{2}$$

4. Flexibility distribution model

The tangent stiffness and flexibility matrices of the two end sections are denoted S_j, D_j, respectively. The subscript j is equal 1 for the left end section and 2 for the right end section. The two matrices are defined as:

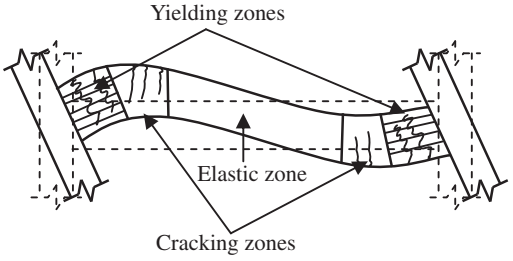

Figure 2 Deformed RC member.

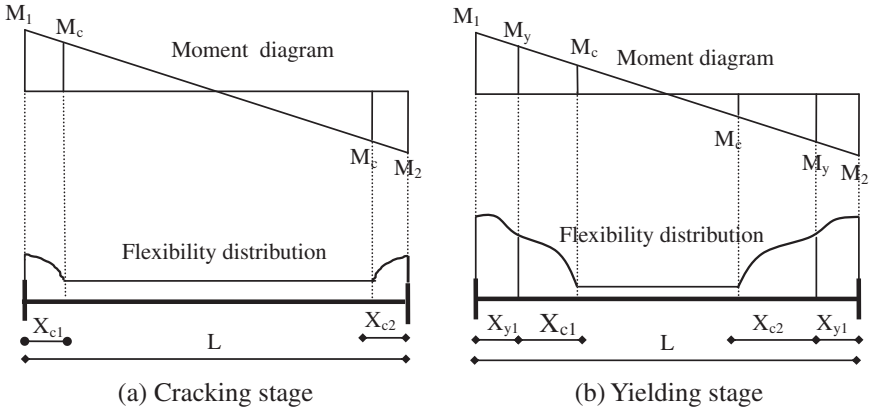

Figure 3 Yielding and cracking lengths.

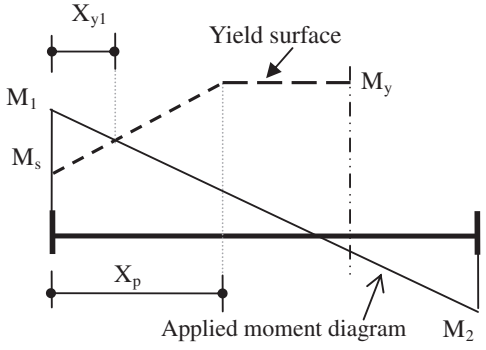

Figure 4 Yielding length calculations.

$$S_j = \begin{bmatrix} s_{1,j} & s_{2,j} \\ s_{2,j} & s_{3,j} \end{bmatrix}, \quad D_j = \begin{bmatrix} d_{1,j} & d_{2,j} \\ d_{2,j} & d_{3,j} \end{bmatrix}, \quad (j = 1, 2) \tag{3}$$

The two matrices relate the jth cross section incremental deformation vector $\{d\varepsilon_j, d\phi_j\}$ with the jth cross section incremental force vector $\{dp_j, dm_j\}$. Where, $d\varepsilon_j$ is the axial strain increment at the center of the cross section, $d\phi_j$ is the cross section curvature increment, dp_j is the axial force increment and dm_j is the moment increment. The stiffness coefficients $s_{1,j}$, $s_{2,j}$, $s_{3,j}$ are calculated as:

$$s_{1,j} = \sum_{k=1}^{N_{fib}} E_{k,j} A_{k,j} \quad s_{2,j} = \sum_{k=1}^{N_{fib}} E_{k,j} A_{k,j} Y_{k,j}$$
$$s_{3,j} = \sum_{k=1}^{N_{fib}} E_{k,j} A_{k,j} Y_{k,j}^2, \quad (j = 1, 2) \tag{4}$$

where $A_{k,j}$, $E_{k,j}$ and $Y_{k,j}$ are the area, the tangent modulus of elasticity and the Y-coordinate of the kth fiber at the jth end section. N_{fib} is the total number of fibers over the end section. The tangent flexibility matrix D_j is obtained by inverting the tangent stiffness matrix S_j. The coefficients $d_{1,j}$, $d_{2,j}$ and $d_{3,j}$ are the axial, the combined and the flexural flexibility coefficients, respectively, at the jth end section of the element.

Cross sections along the element length exhibit different levels of flexibilities, depending on the extent of the experienced inelasticity. The distributions of the flexibility coefficients along the element length are defined using six yielding flexibility distribution functions $FY_{i,j}$ and other six cracking flexibility distribution functions $FC_{i,j}$ as shown in Fig. 5. The subscript i is equal to 1 for the axial flexibility, 2 for the combined flexibility and 3 for the flexural flexibility. The distribution functions relate the values of the flexibility coefficients (the function output) with the distance variable x or x'' (the function input). The lengths of the flexibility distribution shapes are the cracking and the yielding lengths (X_{cj} and X_{yj}), as shown in Fig. 5.

The heights of the flexibility distribution functions $FY_{i,j}$ are defined by $(d_{i,j} - d_{i,j}^c)$ as shown in Fig. 5. The flexibility coefficients $d_{i,j}^c$ are the flexibility coefficients of the end sections at the end of the cracking stage and just before yielding of the reinforcement. The heights of the flexibility distribution functions $FC_{i,j}$ are defined by $(d_{i,j}^c - d_{i,0})$. $d_{i,0}$ represents the ith flexibility coefficient of the elastic part of the beam-column member ($d_{1,0} = 1/EA_o$ and $d_{3,0} = 1/EI_o$), where, E is the member modulus of elasticity, A_o is the member cross section area and I_o is the moment of inertia of the member cross section. The combined flexibility coefficient $d_{2,0}$ is equal to zero for elastic cross

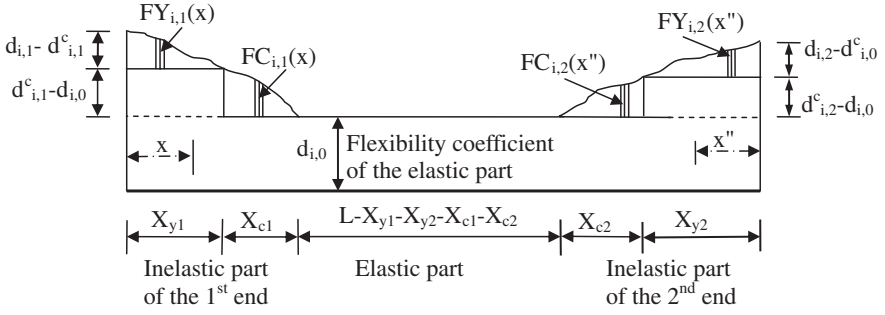

Figure 5 Flexibility distribution functions along the beam-column element.

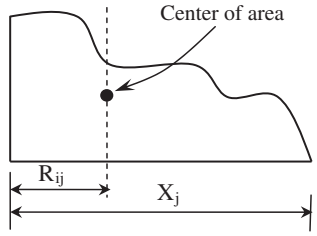

Figure 6a General flexibility shape.

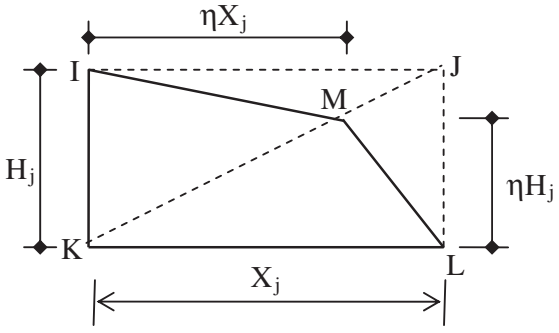

Figure 6b Simplified flexibility diagram.

sections. Also, it is equal to zero in case of using a variable reference axis that coincides with the neutral axis of the cross section. In the current study, the reference axis is kept constant during the analysis which results in nonzero values of the combined flexibility coefficient during the inelastic stage.

Abou-Elfath [15] reported that all the information related to a general flexibility shape that is required for deriving the member flexibility matrix are the length, the height and three shape constants C_1, C_2 and C_3. The constants C_1, C_2 and C_3 are related to the area of the flexibility distribution shape ($A_{i,j}$), the distance between the center of the flexibility shape and the nearest member end ($R_{i,j}$) as shown in Fig. 6a, and the inertia of the flexibility shape about a central axis perpendicular to the beam-column element ($I_{i,j}$). Assuming that all the flexibility functions of the beam-column element have identical shape constants then the shape constants can be estimated as:

$$C_1 = \frac{A_{i,j}}{X_j(d_{i,j} - d_{i,0})}, \quad C_2 = \frac{R_{i,j}}{X_j}, \quad C_3 = \frac{I_{i,j}}{A_{i,j}X_j} \tag{5}$$

Abou-Elfath [15] proposed the bilinear flexibility diagram shown in Fig. 6b to represent the flexibility distributions of beam-column elements. The proposed bilinear shape is defined by the broken line *I–M–L* using the flexibility factor η. The flexibility factor η defines the position of the middle point *M*. The point *M* coincides with the point *J* when $\eta = 1.0$, while it coincides with the point *K* when $\eta = 0$. The value of the flexibility factor η ranges from zero to one. The value of one corresponds to uniform flexibility distribution shape, the value of zero corresponds to zero flexibility distribution shape, while the value of 0.5 corresponds to linear flexibility distribution shape. The flexibility constants can be calculated as:

$$C_1 = \eta, \quad C_2 = (1 + 2\eta)/6, \quad C_3 = (2 - \eta + 2\eta^2)/36 \tag{6}$$

The flexibility factor η provides tremendous number of flexibility distribution selections that are expected to approximately fit any actual flexibility distribution shape. Table 1 summarizes the values of the shape constants corresponding to some levels of the flexibility factor η.

5. Material models

The most commonly used non-linear stress–strain relationship of concrete in tension comprises of a linearly elastic relationship before cracking and a linear descending branch beyond cracking to represent the tension stiffening as shown in Fig. 7a. In this figure, f_{cr} and ε_{cr} are the cracking stress and strain, respectively. The concrete cracking stress is calculated using the equation proposed by Balakrishnan and Murray [16], while the initial tangent modulus, E_1, is considered equal to the initial tangent modulus in compression. The maximum tensile strain ε_{ut} at which the concrete tensile stress is assumed to be zero is assumed equal to $\alpha\varepsilon_{cr}$, where α is considered equal to 10 as proposed by Lee and Mosalam [17]. It is assumed that a fiber with its tensile strain $\geqslant 10\varepsilon_{cr}$ is fully cracked and has completely lost its tensile strength.

The stress–strain relationship of confined concrete in compression (Fig. 7b) is represented using the tri-linear approximation of Elmorsi [18], which is based on the stress–strain relation proposed by Saenz [19]. In this figure, ε'_c and f'_c are the peak strain and stress of the unconfined concrete. The value of f'_c is usually known while the value of ε'_c is estimated using the formula proposed by Al Sulayfani and Lamirault [20]. The initial tangent stiffness E_1 is equal to $2f'_c/\varepsilon'_c$. K is the factor that accounts for the strength increase due to confinement. The factor *K* and the slope of the strain softening branch of the compression stress–strain relationship are dependent on the amount of steel stirrups and are calculated using the model of Kent and Park [21].

The rules that govern the cyclic behavior of concrete in compression are considered as those presented by Taucer et al. [11]. Unloading from a point on the envelope curve takes place along a straight line connecting the point ε_r at which unloading starts to a point ε_p on the strain axis. The value of ε_p is given by the equations proposed by Karasan and Jirsa [22] and modified by Taucer et al. [11].

Table 1 Shape constants corresponding to some levels of η.

η	C_1	C_2	C_3	η	C_1	C_2	C_3
0.10	0.10	0.2000	0.0533	0.60	0.60	0.3667	0.0589
0.20	0.20	0.2333	0.0522	0.70	0.70	0.4000	0.0633
0.30	0.30	0.2667	0.0522	0.80	0.80	0.4333	0.0689
0.40	0.40	0.3000	0.0533	0.90	0.90	0.4667	0.0756
0.50	0.50	0.3333	0.0555	1.00	1.00	0.5000	0.0833

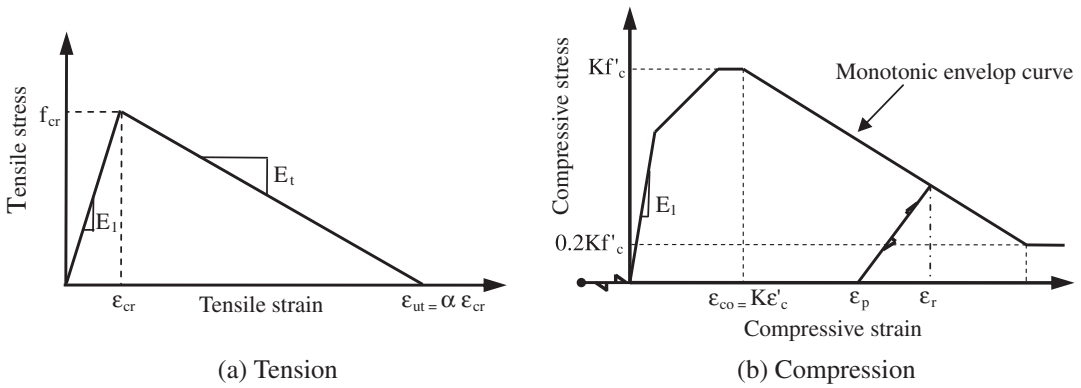

Figure 7 Concrete stress–strain relationships.

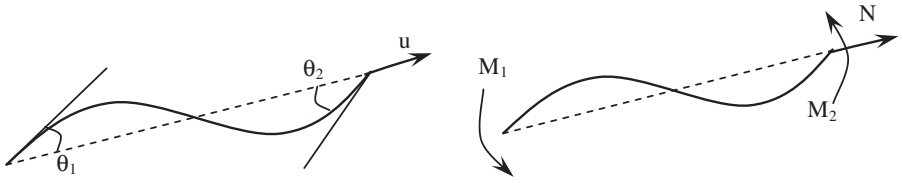

Figure 8 Deformation and force components of the beam-column model.

The monotonic response of reinforcing steel is represented using a bilinear elastic-strain hardening model which is widely used for its simplicity. A kinematic hardening rule is considered for modeling the cyclic stress–strain relation of the reinforcing steel.

6. Member flexibility matrix

The beam-column model has three local degrees of freedom $\{u, \theta_1, \theta_2\}$ and three local force components $\{N, M_1, M_2\}$, as shown in Fig. 8. θ_1 and θ_2 represent the nodal rotations, u represents the axial displacement, M_1 and M_2 represent the member end moments and N represents the axial force. The incremental displacement vector and the incremental force vector of the element are related by a symmetric tangent flexibility matrix in local coordinates according to:

$$\begin{Bmatrix} du \\ d\theta_1 \\ d\theta_2 \end{Bmatrix} = \begin{bmatrix} F_{11} & F_{12} & F_{13} \\ F_{21} & F_{22} & F_{23} \\ F_{31} & F_{32} & F_{33} \end{bmatrix} \begin{Bmatrix} dN \\ dM_1 \\ dM_2 \end{Bmatrix} \tag{7}$$

$$\text{Or in general form}: \ \{d\delta\} = [F]\{dP\} \tag{8}$$

The data required for determining the tangent flexibility matrix $[F]$ are the tangent flexibility coefficients of the end sections $d_{i,j}$, the tangent flexibility coefficients of the end sections at the end of the cracking stage $d^c_{i,j}$, the yielding and the cracking lengths (X_{c1}, X_{y1}, X_{c2} and X_{y2}), the flexibility distribution functions considered along the inelastic lengths, and the member elastic properties (EA_o, EI_o and L). The shape constants assigned for the yielding flexibility functions are denoted C_{y1}, C_{y2}, and C_{y3}, while the shape constants considered for the cracking zones are denoted C_{c1}, C_{c2}, and C_{c3}.

The flexibility coefficients F_{ij} are calculated using the elastic weight method. In the elastic weight method, the flexibility coefficients F_{ij} are the local reactions of the beam-column element when loaded with elastic loads which obtained by integrating the flexibility distribution diagrams shown in Fig. 5 with the internal force diagrams shown in Fig. 9. The flexibility coefficients F_{ij} are calculated as follows:

$$\begin{aligned}
F_{11} &= L/EA_0 + A_{11} + B_{11} + C_{11} + A_{12} + B_{12} + C_{12} \\
F_{12} &= A_{21}(1 - Zy1) + B_{21}(1 - X_{y1}/2L) + C_{21}(1 - Zc1 - X_{y1}/L) + A_{22}Z_{y2} \\
&\quad + B_{22}X_{y2}/2L + C_{22}(X_{y2}/L + Z_{c2}) \\
F_{13} &= -A_{21}Zy1 - B_{21}(X_{y1}/2L) - C_{21}(X_{y1}/L + Z_{c1}) - A_{22}(1 - Z_{y2}) \\
&\quad - B_{22}(1 - X_{y2}/2L) - C_{22}(1 - X_{y2}/L - Z_{c2}) \\
F_{22} &= L/3EI + A_{32}Z_{y2}W_{y2} + B_{32}(X_{y2}/L)^2/3 + C_{32}((X_{y2}/L)^2 \\
&\quad + Z_{c2}(2X_{y2}/L + W_{c2})) + A_{31}(1 - Z_{y1}(2 - W_{y1})) \\
&\quad + B_{31}(1 - X_{y1}/L + (X_{y1}/L)^2/3) + C_{31}((1 - X_{y1}/L)^2 + Z_{c1}(-2 + 2X_{y1}/L + W_{c1})) \\
F_{23} &= -L/6EI - A_{32}Z_{y2}(1 - W_{y2}) - B_{32}(X_{y2}/2L - (X_{y2}/L)^2/3) - C_{32}(X_{y2}/L - (X_{y2}/2)^2 \\
&\quad + Z_{c2}(1 - 2X_{y2}/L - W_{c2})) - A_{31}Z_{y1}(1 - W_{y1}) - B_{31}(X_{y1}/2L - (1/3)(X_{y1}/L)^2) \\
&\quad - C_{31}(X_{y1}/L - (X_{y1}/L)^2) + Z_{c1}(1 - 2X_{y1}/L - W_{c1})) \\
F_{33} &= L/3EI + A_{31}Z_{y1}W_{y1} + B_{31}(X_{y1}/L)^2/3 \\
&\quad + C_{31}((X_{y1}/L)^2 + Z_{c1}(2X_{y1}/L + W_{c1}))A_{32}(1 - Z_{y2}(2 - W_{y2})) \\
&\quad + B_{32}(1 - X_{y2}/L + (X_{y1}/L)^2/3) + C_{32}((1 - X_{y2}/L)^2 \\
&\quad + Z_{c2}(-2 + 2X_{y2}/L + W_{c2}))
\end{aligned} \tag{9}$$

where

$$A_{,ij} = C_{y1}X_{yj}(d_{ij} - d^c_{ij}), \quad B_{ij} = X_{yj}(d^c_{ij} - d_{i0}), \quad C_{ij} = C_{c1}X_{cj}(d^c_{ij} - d_{i0})$$
$$Z_{yj} = C_{y2}X_{yj}/L, \quad Z_{cj} = C_{c2}X_{cj}/L, \quad W_{cj} = (C_{c2} + C_{c3}/C_{c2})X_{cj}/L,$$
$$W_{yj} = (C_{y2} + C_{y3}/C_{y2})X_{yj}/L \tag{10}$$

Eqs. (9) and (10) indicate that the flexibility shapes are represented in the element tangent flexibility matrix only by the inelastic lengths (X_{y1}, X_{y2}, X_{c1}, and X_{c2}), flexibility coefficients

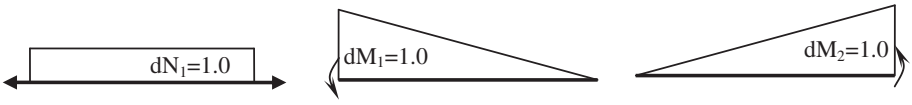

Figure 9 Diagrams of unit force increments.

of the end sections ($d_{i,j}$ and $d^{c}_{i,j}$), the flexibility constants of the yielding and the cracking shapes (C_{y1}, C_{y2}, C_{y3}, C_{c1}, C_{c2}, and C_{c3}). In case of neglecting the concrete tensile strength for the purpose of simplicity, the flexibility coefficients can be calculated as:

$$\begin{aligned} F_{11} &= L/EA_{cr} + A_{11} + A_{12}F_{12} = A_{21}(1 - Z_1) + A_{22}Z_2 \\ F_{13} &= -A_{21}Z_1 - A_{22}(1 - Z_2) \\ F_{22} &= L/3EI_{cr} + A_{31}(1 - 2Z_1 + Z_1W_1) + A_{32}Z_2W_2 \\ F_{23} &= -L/6EI_{cr} + A_{31}Z_1(W_1 - 1) + A_{32}Z_2(1 - W_2) \\ F_{33} &= L/3EI_{cr} + A_{31}Z_1W_1 + A_{32}(1 - 2Z_2 + Z_2W_2) \end{aligned} \tag{11}$$

where A_{cr} and I_{cr} are the area and the moment of inertia of the cracked cross section and:

$$\begin{aligned} A_{ij} = C_{y1}X_{yj}(d_{ij} - d_{i0}), \quad Z_j = C_{y2}X_{yj}/L, \\ W_j = (C_{y2} + C_{y3}/C_{y2})X_{yj}/L \end{aligned} \tag{12}$$

Eqs. (11) and (12) indicate that the flexibility shapes are represented in the element inelastic flexibility matrix by only the yielding lengths (X_{y1} and X_{y2}), the flexibility values of the end sections ($d_{i,j} - d_{i,0}$) and the shape constants (C_{y1}, C_{y2} and C_{y3}). The equations also indicate that the proper estimation of the shape constants is a crucial issue for accurately determining the inelastic response of the RC members.

7. Conclusions

The proposed RC beam-column model formulated in this study strikes a good balance between accuracy and simplicity. The simplicity of the proposed model is achieved by monitoring only the responses of the end sections and eliminating the need for considering many segments along the element length.

The response of the end sections is calculated by dividing them into concrete and steel fibers. The material model used for concrete is simple for programming and takes into account the main behavioral characteristics of concrete under the effect of cyclic loading. The inelastic zones at the member ends are divided into cracking and yielding zones with their lengths are updated every load increment. The overall response of the member is estimated using a preset flexibility distribution functions along the element length. The preset flexibility distribution functions are selected to fit the actual flexibility distributions.

The proposed model accounts rationally for the axial–flexural interaction and provides the fiber strains as an output which can be used for in seismic damage evaluation of RC members. Moreover, the model accounts for the spread of plasticity and is capable of producing the gradual change of the stiffness in the post-yield range. The proposed beam-column element is implemented in the general purpose computer program DRAIN-2DX.

References

[1] R.W. Clough, K.L. Benuska, E.L. Wilson, Inelastic earthquake response of tall buildings, in: Proceedings 3rd World Conference on Earthquake Engineering, New Zealand, 1965, pp. 11.
[2] M.F. Giberson, Two nonlinear beams with definitions of ductility, Journal of the Structural Division, ASCE 95 (ST2) (1969).
[3] T. Takeda, M.A. Sozen, N. Nielsen, Reinforced concrete response to simulate earthquakes, Journal of Structural Division, ASCE 96 (St 12) (1970) 2557–2573.
[4] R. Park, D.C. Kent, R.A. Sampson, Reinforced concrete members with cyclic loading, Journal of the Structural Division, ASCE 98 (ST7) (1972).
[5] S. Otani, Inelastic analysis of R/C frame structures, Journal of the Structural Division, ASCE 100 (ST7) (1974) 1433–1449.
[6] S.S. Lai, G.T. Will, S. Otani, Model for inelastic biaxial bending of concrete members, Journal of Structural Engineering, ASCE 110 (11) (1984).
[7] M. Saiidi, G. Ghusn, Y. Jiang, Five-spring element for biaxially bent R/C columns, Journal of Structural Engineering, ASCE 115 (2) (1989).
[8] C. Meyer, M.S. Roufaiel, S.G. Arzoumanidis, Analysis of damaged concrete frames for cyclic loads, Earthquake Engineering and Structural Dynamics 11 (1983) 207–228.
[9] M.S.L. Roufaiel, C. Meyer, Analytical modeling of hysteretic behavior of R/C frames, Journal of Structural Engineering, ASCE 113 (3) (1987).
[10] Y.J. Park, A.M. Reinhorn, S.K. Kunnath, IDARC 2D: Inelastic Damage Analysis of Reinforced Concrete Frame – Shear-Wall Structures, Technical Report NCEER-87-0008, State University of New York at Buffalo, 1987.
[11] F.F. Taucer, E. Spacone, F.C. Filippou, A Fiber Beam-Column Element For Seismic Response Analysis of Reinforced Concrete Structures. Report No. UCB/EERC-91/17, Earthquake Eng. Research Center, University of California at Berkeley, CA, 1991.
[12] S.A. Kaba, S.A. Mahin, Refined Modeling of Reinforced Concrete Columns for Seismic Analysis, Report No. UBC/EERC-84/3, University of California at Berkeley, CA, 1984.
[13] V. Prakash, G.H. Powell, DRAIN-2DX-Version 1.02 – User Guide, Report No. UCB/SEMM-93/17, Civil Eng. Dept., University of California at Berkeley, CA, 1993.
[14] H.M. Abou-Elfath, A new beam-column model for seismic analysis of steel frame buildings, in: Sixth International Conference, vol. 3, Al-Azhar Engineering, Cairo, 2000, pp. 220–230.
[15] H.M. Abou-Elfath, A new flexibility distribution model for beam-column elements used in seismic analysis of steel frame buildings, Alexandria Engineering Journal 47(1) (2008) (Faculty of Engineering, Alexandria University, Egypt).
[16] S. Balakrishnan, D.W. Murray, Concrete constitutive model for NLFE analysis of structures, Journal of Structural Engineering, ASCE 114 (7) (1988) 1449–1466.
[17] T.H. Lee, K.M. Mosalam, Probabilistic fiber element modeling of reinforced concrete structures, Computers and Structures 82 (2004) 2285–2299.
[18] M.S.-E. Elmorsi, Analytical Modeling of Reinforced Concrete Beam Column Connections for Seismic Loading, Ph.D. Thesis, McMaster University, Hamilton, Ontario, Canada, 1998.

[19] L.P. Saenz, Equation for the stress–strain curve of concrete, Journal of the American Concrete Institute 61 (9) (1964) 1229–1235 (Discussion).

[20] B. Al Sulayfani, J. Lamirault, Contribution à L'analyse Expérimentale du Comportement Mécanique Cyclique du Béton, Materials and Structures/Materaux et Constructions 20 (118) (1987) 283–292 (in French).

[21] D.C. Kent, R. Park, Flexural members with confined concrete, Journal of the Structural Division, ASCE 97 (ST7) (1990) 1969–1990.

[22] I.D. Karsan, J.O. Jirsa, Behavior of concrete under compressive loadings, Journal of the Structural Division ASCE 95 (ST12) (1969) 2543–2563.